Amino Acids (2013) 44:933–946
DOI 10.1007/s00726-012-1423-7

ORIGINAL ARTICLE

Synthesis, characterization, conformational analysis of a cyclic conjugated octreotate peptide and biological evaluation of ^{99m}Tc-HYNIC-His^3-Octreotate as novel tracer for the imaging of somatostatin receptor-positive tumors

Ashok Behera · Indranil Banerjee · Kakali De · Rudra Narayan Munda · Sankha Chattopadhayay · Amalesh Samanta · Bharat Sarkar · Santanu Ganguly · Mridula Misra

Received: 28 June 2012 / Accepted: 12 October 2012 / Published online: 23 October 2012

Abstract Peptides are attracting increasing interest in nuclear oncology for targeted tumor diagnosis and therapy. We therefore synthesized new cyclic octapeptides conjugated with HYNIC by Fmoc solid-phase peptide synthesis. These were purified and analyzed by RP-HPLC, MALDI mass, ^{1}H NMR, ^{13}C NMR, HSQC, HMBC, COSY and IR spectroscopy. Conformational analysis of the peptides was performed by circular dichroism spectroscopy, in pure water and trifluoroethanol–water (1:1), revealed the presence of strong secondary structural features like β-sheet and random coils. Labeling was performed with ^{99m}Tc using Tricine and EDDA as coligands by $SnCl_2$ method to get products with excellent radiochemical purity >99.5 %. Metabolic stability analysis did not show any evidence of breaking of the labeled compounds and formation of free ^{99m}Tc. Internalization studies were done and IC_{50} values were determined in somatostatin receptor-expressing C6 glioma cell line and rat brain cortex membrane, and the results compared with HYNIC-TOC as standard. The IC_{50} values of ^{99m}Tc-HYNIC-His^3-Octreotate (21 ± 0.93 nM) and ^{99m}Tc-HYNIC-TOC (2.87 ± 0.41 nM) proved to be comparable. Biodistribution and image study on normal rat under gamma camera showed very high uptake in kidney and urine, indicating kidney as primary organ for metabolism and route of excretion. Biodistribution and image study on rats bearing C6 glioma tumor found high uptake in tumor (1.27 ± 0.15) and pancreas (1.71 ± 0.03). Using these findings, new derivatives can be prepared to develop ^{99m}Tc radiopharmaceuticals for imaging somatostatin receptor-positive tumors.

Keywords Solid-phase peptide synthesis · SSTR · Binding affinity · C6 glioma cell · Internalization study

Abbreviations

DIPEA	Diisopropylethylamine
DMF	Dimethylformamide
TBTU	2-(1H-Benzotriazole-1-yl)-1,1,3,3-tetramethyluronium tetrafluoroborate hexafluorophosphate
SPPS	Solid-phase peptide synthesis
TNBS	Picryl sulfonic acid
HYNIC	Hydrazinonicotinic acid
GPCRs	G-protein-coupled membrane receptors
SPECT	Single-photon emission computed tomography
DMEM	Dulbecco's modified eagle medium

Electronic supplementary material The online version of this article (doi:10.1007/s00726-012-1423-7) contains supplementary material, which is available to authorized users.

A. Behera · I. Banerjee · K. De · R. N. Munda · M. Misra (✉)
Department of Nuclear Medicine, Infectious Disease and Immunology Division, CSIR-Indian Institute of Chemical Biology, 4, Raja S.C. Mullick Road, Kolkata 700032, India
e-mail: mridulamisra@iicb.res.in

A. Behera
e-mail: ashubehu2000@gmail.com

S. Chattopadhayay
Radiopharmaceuticals Laboratory, Regional Centre, Board of Radiation and Isotope Technology, Variable Energy Cyclotron Centre, 1/AF, Bidhan Nagar, Kolkata 700 064, India
e-mail: sankha@vecc.gov.in

A. Samanta
Department of Pharmaceutical Technology, Jadavpur University, Kolkata 700032, India

B. Sarkar · S. Ganguly
Regional Radiation Medicine Centre, Thakurpukur Cancer Research Centre, Kolkata 700 063, India

Introduction

Today peptides play an essential role in almost any field of medicine, particularly in nuclear medicine and radio pharmacy (Liu et al. 1997; Liu and Edwards 1999). Somatostatin (SST) is a regulatory cyclopeptide hormone and its biological effects are mediated via specific high affinity GPCRs. Five distinct subtypes of somatostatin receptors (SSTRs) have been identified (SSTR 1–SSTR 5) and cloned (Koenig et al. 1996, 1997). SSTRs are over expressed in homogenous and heterogeneous manners in the majority of tumors like neuroendocrine tumors (NETs), small cell lung cancer, breast cancer, gliomas and lymphoma (Breeman et al. 2001; Nikolopoulou et al. 2006). The native hormone is, however, susceptible to rapid enzymatic degradation ($t_{1/2}$ = 2–3 min in blood) and is, therefore, unsuitable for in vivo applications. For this purpose, long-lived synthetic octapeptide analogs have been developed such as octreotide, octreotate and their derivatives. Therefore, it is of high interest to find a specific SPECT tracer for the imaging of SSTR expression in tumors.

Like proteins and antibodies, small synthetic peptides are currently the agents of choice for tumor imaging because of their favorable pharmacokinetic characteristics such as rapid clearance from blood and non-targeted tissues (Liu and Edwards 1999; Fischman et al. 1993). Radiopharmaceuticals labeled with ^{67}Ga, ^{111}In, ^{90}Y and various iodine isotopes have been in use for a much longer time, but beside these short-lived radionuclides, radiopharmaceuticals labeled with ^{99m}Tc are in demand both for economic reasons and favorable imaging characteristics of technetium (γ energy of 140 keV and 6 h half-life). Several attempts for the preparation of ^{99m}Tc-labeled somatostatin analogs prepared over the last decade, where labeling was done via HYNIC for improved tumor targeting and body clearance, have met with varying degrees of success. Despite the ease and convenience of direct labeling of the peptides with ^{99m}Tc, it usually results in poor stability of the ^{99m}Tc–peptide complexes due to the lack of control over chelate metal non-specific binding.

To overcome this problem, a wide variety of bifunctional chelating moieties or agents have been proposed for incorporation in the peptide ligand for facile preparation of peptide-based radiopharmaceuticals. Maximizing the retention of radioactivity at the tumor site is an important consideration in the development of the labeled peptide as targeted radiopharmaceutical. Receptor-mediated internalization can increase the residence time of the radionuclide in tumor cells if the labeled molecule is charged, because the lipophilic lysosomal and cell membranes provide a barrier for escape into the extracellular environment. It appears that increasing the polarity of the COOH and NH_2 terminus of the peptide can result in higher levels of internalized activity (Vaidyanathan et al. 2003). To facilitate the interpretation of results, the peptides in the present study were designed by replacing the Phe residue at position 3 with Tyr and His (to decrease lipophilicity) and the COOH-terminal threoninol with threonine to provide an additional negative charge on HYNIC-His^3-Octreotate molecule. The effects of modification on internalization and retention activity were then investigated on rat model developing with C6 glioma tumor. We present the synthesis, characterization, conformational analysis, radiolabeling and biological evaluation of ^{99m}Tc-labeled cyclic conjugated peptides as novel tracer for the imaging of SSTR-positive tumors.

Materials and methods

All amino acid derivatives and resins for the synthesis of novel somatostatin analogs were purchased from Nova-Biochem (Switzerland). All other reagents and solvents were obtained from Sigma-Aldrich or Merck, Germany or from SRL, India. The prochelator HYNIC-Boc was synthesized according to Abrams et al. (1990) with slight modification. Sodium pertechnetate ($Na^{99m}TcO_4$) was obtained from commercial ^{99}Mo/^{99m}Tc generator (Radioisotope Division, BARC, Mumbai).

^{1}H and ^{13}C NMR spectra were acquired with a Bruker DRX 600 MHz NMR instruments at ambient temperature. Chemical shifts are reported in parts per million (ppm) relative to D_2O as internal standard. IR spectra were recorded on a JASCO-FTIR Model-410, using KBr pellets. Mass spectra were recorded on an Applied Biosystems 4700 proteomics analyzer 170. The CD spectra have been recorded on a Jasco J815 spectropolarimeter. High-performance liquid chromatography (HPLC) analysis and purification of peptides were performed on a Shimadzu HPLC system using two LC20AD solvent pumps and an SPD-M20A prominence diode array detector. Injections of 300 µl were made on a μbondapak C-18, 10 µm, 125 Å, 7.8 × 300 mm reverse-phase column. The compounds were eluted from the column at a flow rate of 1 ml/min using a gradient system consisting of 0.1 % trifluoroacetic acid (TFA)/water (solvent A) and 0.085 % TFA/acetonitrile (solvent B). A 32-min binary gradient was used. Gradient I: 0 min 100 % A (0 % B), 5 min 80 % A (20 % B), 10 min 65 % A (35 % B), 15 min 50 % A (50 % B), 25 min 20 % A (80 % B), 30 min 0 % A (100 % B), 32 min 100 % A (0 % B). The column effluent was monitored using a UV detector set at 254 nm. The radiochemical purity assessment and quality control of radiolabeled peptides were achieved using silica gel plates (ITLC-SG, Merck), and HPLC technique was used to

validate ITLC approach. The radiochemical purity of labeled peptides was determined by HPLC (Waters) with reversed-phase C18 column (4.6 × 250 mm, μbondapak column from Waters). The mobile phase used in RP-HPLC for gradient system consisted of 0.1 % TFA/water (solvent A), 0.85 % TFA/acetonitrile (solvent B) and flow rate was 1 ml/min. Gradient II: 0 min 100 % A (0 % B), 2 min 90 % A (10 % B), 6 min 80 % A (20 % B), 12 min 50 % A (50 % B), 25 min 10 % A (90 % B), 35 min 90 % A (10 % B), 45 min 100 % A (0 % B). The solvents used for ITLC were 2-Butanone, 0.1 M sodium citrate pH 5.1 and methanol/1 M ammonium acetate (1:1) separately. Strips were analyzed in a well-type gamma counter. Radioactivity counting for biodistribution studies was done using a quantitative gamma counter in NaI(TI) well crystal, gamma ray spectrometer: GRS 23C, ECIL. The results were corrected for background radiation and physical decay during counting.

Synthesis of HYNIC-conjugated peptides

Octreotide analog HYNIC-His^3-Octreotate (**1**) and the standard HYNIC-TOC (**2**) were semi-automatically synthesized on a peptide synthesizer (PS3 Protein Technology Instruments, NULAB, USA) followed by standard Fmoc SPPS on H-Thr(tBu)-2-chlorotrityl resin (substitution 0.30–0.90 mmol/g) for **1** and, for **2**, the synthesis was described in our previous report (Behera et al. 2011). Fmoc-protected amino acids were activated in situ in AA cartridges with TBTU/DIPEA in DMF. Coupling of each amino acid was performed in the presence of 10 mol excess of Fmoc-amino acid, 9.5 mol excess TBTU, and 20 mol excess of DIPEA in DMF. Amino acids were coupled by removing Fmoc-protecting groups with 20 % piperidine/DMF for 10 min followed by washing with DMF. Progress of the amino acid coupling was monitored by color change of picryl sulfonic acid (TNBS). This process was repeated until the required sequence was achieved. Finally, coupling of prochelator to peptide for compounds **1** and **2** was performed in the presence of 5 mol excess of HYNIC-BOC, 4.5 mol excess of TBTU and 10 mol excess of DIPEA in DMF for 40 min; coupling success was checked by TNBS test. The coupled resin was filtered and rinsed with DMF. The average coupling yield was calculated from the increase in weight of the elongated peptide–resin divided by the weight of protected peptide.

Disulfide bond formation and deprotection of peptides

The peptide chain was cyclized (Lee et al. 1998) by formation of cys–cys disulfide bond in solid phase. A part (100 mg) of the peptide–resin was suspended in DMF for 2 h at 25 °C. Then, this peptide–resin solution was added drop wise to a vigorously stirred solution of 10-eq iodine (70 mg) in DMF. After a reaction time of 2 h at 25 °C, excess iodine was washed with DMF to remove the iodine color, and the resin was washed with ether and dried. The S–S cyclized peptide chains with all protecting groups were cleaved by treatment with 95 % TFA, 0.5 % thioanisole, 2.5 % ethane dithiol (EDT) and 2.5 % water at 25 °C for 3–4 h. Then, it was rinsed with DMF and the crude product was precipitated with cold diethyl ether.

Purification, characterization and structure elucidation of peptide

Finally, the crude peptide was purified and analyzed on a semi-preparative HPLC system equipped with C18 column using gradient I as solvent system. The major peak at retention time of 22.095 min for peptide **1** was collected. Then, it was lyophilized and stored at −20 °C freezer. Next, the purified product was characterized by matrix-assisted laser desorption ionization (MALDI) spectrometry in positive-ion mode. The structure of peptide was then elucidated by 1D NMR (^{1}H NMR, ^{13}C NMR, DEPT 90, 135), 2D NMR (HSQC, HMBC, COSY) and FT-IR spectroscopy. The peptide was quantitated by amino acid analysis of a 24-h acid hydrolysate using Waters Accu-Tag chemistry together with a Waters HPLC system.

Circular dichroism (CD) spectroscopy

The CD spectra were recorded on a Jasco J815 spectropolarimeter (Jasco International Co., Ltd. Hachioji, Japan) equipped with a peltier cell holder and temperature controller PFD425 L/15 for monitoring the conformational changes of the HYNIC-conjugated peptides in H_2O and TFE:H_2O (1:1) in the range of 190–250 nm. The peptide concentration and path length of the cell used were 865 μM and 0.1 cm, respectively, for far UV CD. The instrument parameters for CD measurements were scanning speed of 50 nm/min, bandwidth of 1.0 nm, and sensitivity of 100 millidegree. Five scans were averaged and smoothed to improve signal-to-noise ratio. Secondary structure analysis was performed by the software supplied by Jasco.

^{99m}Tc labeling and radiochemical analysis

Radiolabeling (Lee et al. 1998; Decristoforo et al. 2000b; von Guggenberg et al. 2006; Behera et al. 2011) of HYNIC-conjugated peptide with ^{99m}Tc was performed using $SnCl_2{\cdot}2H_2O$ (25 μg) as reducing agent and ethylenediamine *N*,*N* diaceticacid (EDDA, 10 mg in 0.5 ml 0.1 N NaOH) with Tricine (20 mg in 0.5 ml distilled water) as coligands to stabilize ^{99m}Tc bound to the hydrazino residue of the peptide conjugates (20 μg). Labeling of conjugated peptide

with ^{99m}Tc was performed using various activities of ^{99m}Tc (37–370 MBq) and incubated for 20 min at 100 °C. Radiochemical purity of radiolabeled peptides was validated by ITLC and RP-HPLC using gradient II as solvent system.

In vitro serum stability study

In vitro stability of the radiolabeled peptide complex was studied by the method reported by Behera et al. (2011). Briefly, 0.5 ml of rat serum was mixed with 0.2 ml of ^{99m}Tc-HYNIC-His^3-Octreotate (**3**) in a vial and incubated at 37 °C. A part (10 µL) of the solution was taken out from the sample at time intervals of 1, 2, 4, 6, 8, 12 and 24 h at room temperature and assessed by ITLC method to determine the percentage of radiolabeled complex and free pertechnetate. The stability of radiolabeled peptides was validated by RP-HPLC using gradient II as solvent system at different time intervals.

Metabolic stability in rat kidney and urine

Rats were prepared according to the procedure described for the biodistribution studies. After 15 min and 120 min of the bolus injection of ^{99m}Tc-peptides (37 MBq), the animals were sacrificed to collect urine and kidney samples. Kidneys were homogenized and centrifuged at 10,000 rpm for 10 min to collect the supernatant. The supernatant was dried and aliquots from the supernatant were analyzed by HPLC for metabolites applying the same conditions as for radiolabeled peptides. Retention times (R_t) obtained from the above experiment were compared with the specified R_t value of complex **3**. The urine sample, which was collected from the bladder with a syringe, was also centrifuged at 10,000 rpm for 10 min to collect the supernatant. The supernatant was dried and aliquots from the supernatant were analyzed by HPLC for metabolites applying the same conditions as for the radiolabeled peptides.

Cell line and culture condition

C6 glioma cell line was obtained from National centre for cell science (NCCS), Pune, India. C6 glioma cell was grown confluent in DMEM-high glucose nutrient mixture supplemented by 10–20 % (v/v) fetal bovine serum, 1 mM glutamine, 100 U/ml penicillin and 100 µg/ml streptomycin in humidified air containing 5 % CO_2 at 37 °C. Subculturing was performed employing a trypsin/EDTA (0.05/0.02 % w/v) solution.

Membrane preparation

For SSTR binding studies, membrane was prepared from mouse brain (Maina et al. 2002; Gabriel et al. 2004; Mitra et al. 2011). The mouse was sacrificed; the brain was dissected out, homogenized in ice-cold 50 mM Tris–HCl buffer (pH 7.4) and centrifuged at 20,000*g* for 30 min. The pellet was resuspended in the same buffer and incubated for 20 min at 37 °C followed by centrifugation as above. The pellet was resuspended in ice-cold buffer and used for binding assay. Protein concentration was determined by Bradford assay method using bovine serum albumin as standard (Berges et al. 1993).

In vitro receptor binding assays

SSTR binding (Decristoforo et al. 2000b; Mitra et al. 2011; Maina et al. 2002) was carried out with mouse membrane using peptides **1** and **2** as performed earlier. Briefly, membranes (50–60 µg of protein) were incubated with 596 nM of complex **3** for 40 min at 37 °C in 50 mM Tris–HCl buffer, pH 7.4. Non-specific binding was determined in the presence of 0.590 µM concentrations of unlabeled **1** and **2**. Complex **3,** which showed significant affinity for SSTR, was further evaluated for its IC_{50} value using six different concentrations ranging from 1 nM to 25 µM. Following incubation, bound radioligand was collected by filtering under vacuum in a Millipore filtration manifold using glass–fiber filters (GF/B; Whatman, Clifton, NJ), pretreated with 0.5 % polyethyleneimine. The filters were washed thrice with ice-cold buffer and the radioactivities retained on filters were counted in an automatic NaI(TI) gamma counter. The filters were rinsed thoroughly with buffer (4 × 3 ml) and filter activity was measured. Non-specific binding was defined as the amount of activity still bound in the presence of 1 µM cold peptides **1** and **2**. Binding data were analyzed and IC_{50} values were calculated by origin 6.0 software.

Radioligand internalization study

The internalization experiment was performed according to the reported method (Maina et al. 2002, 2006; Gandomkar et al. 2007). Briefly, the C6 glioma cell line-expressing SSTRs were maintained by serial passage in monolayer in DMEM medium in a humidified 5 % CO_2/air atmosphere at 37 °C. For all cell experiments, the cells were seeded at a density of 0.8–1.1 million cells per well in six-well plates and incubated over night with internalization medium. The medium was thereafter removed from the plates and cells were washed once with 2 ml of internalization buffer (DMEM, 1 % fetal bovine serum, amino acids and vitamins, pH 7.4). Fresh aliquot (1.5 ml) of internalization buffer was added to each well and the plates were incubated at 37 °C for about 1 h. About 150 KBq (2.5 pmol per well) of the peptides were then added to the medium and the cells were incubated at 37 °C for the indicated time

periods in triplicates. To determine non-specific membrane binding and internalization, cells were incubated with radioligand in the presence of 1 μmol/l octreotide. Cellular uptake was stopped by removing the medium from the cells and by washing with 1 ml of ice-cold phosphate-buffered saline (PBS). Two acid washes for 10 min each were performed with a 0.1 M glycine buffer of pH 2.8 on ice. Finally, the cells were treated with 1 N NaOH. The culture medium, the bound receptor and the internalized fraction were analyzed radiometrically in a gamma counter.

Biodistribution study on normal and tumor-bearing rats

All the animal experiments were conducted in accordance with the Departmental Committee of Animal Ethics and with the Institutional Guidelines of Indian Institute of Chemical Biology, Kolkata, India for the conduct of experiments on animals. Biodistribution studies for normal rats were performed in Sprague-Dawley rats ($n = 8$; 200–250 gm) and for C6 glioma tumor model was grown in the femur of male Lewis rats (6 weeks old, 100–150 gm) 2–3 weeks after inoculation. Solution of radio complex **3** (200 μCi, 200 μl) alone or together with 100 μg cold HYNIC-TOC (blocked animal) was administered through the femoral vein of anaesthetised rats with 0.5 mm polyethylene (PE) catheter. At different preset time intervals (2, 15, 60 and 120 min for normal rats and 10, 45 min for C6 glioma tumor-developed rats), rats were sacrificed by intravenous injection of air. Blood and urine samples were obtained by puncturing the heart and urinary bladder, respectively. Other organs (brain, heart, liver, lungs, spleen, muscle, kidney, intestine, stomach, tumor and pancreas) were removed, rinsed with saline, and blotted dry to remove the residual blood. The organs were then weighed and radioactivity was counted in a well-type counter (gamma ray spectrometer: GRS 23C, ECIL). Standard counts of the radio complex were also taken and the uptake was expressed in percentage of radioactivity per gram of each organ (% ID/g). The calculations of mean and standard deviation were performed on Microsoft Excel. Student's t test was used to determine statistical significance. Differences at the 95 % confidence level ($p < 0.050$) were considered significant.

Scintigraphic imaging on normal rats and on tumor-bearing rats

Imaging studies were performed on both normal (male Sprague-Dawley rat, 100–150 gm) and tumor-bearing rats at Thakurpukur Cancer Research centre (Regional Radiation Monitoring Centre, Kolkata) under dual-head gamma camera (GE Hawkeyes). The animals were injected via the femoral vein of urethane-anaesthetised rats with a bolus containing complex **3** (200 μCi, 200 μl) alone or together with 100 μg cold HYNIC-TOC (blocked animal) and were sacrificed 1 h p.i. by intravenous injection of air. They were placed in a typical position for planar imaging under a small field of view experimental gamma camera, suitable for both planar and tomographic imaging. Image data were obtained and analyzed using a gamma camera (GE Hawkeyes) fitted with a low energy high-resolution all-purpose collimator using both static and dynamic procedures of the Xeleris (Functional Imaging) Workstation system. The time–activity curves were generated from the above images.

Statistical analysis

All results are expressed as mean ± SEM. The data were analyzed by one-way analysis of variance (ANOVA) followed by Duncan's new multiple range test. Differences with $p < 0.05$ between experimental groups at each point were considered statistically significant.

Results

Synthesis

The prochelator Boc-HYNIC was synthesized from 6-chloronicotinic acid according to Abrams et al. (1990) with slight modification. The peptide sequences were assembled on H-Thr(tBu)-2-chlorotrityl resin for peptide **1**, and O-t-butylthreoninol-2-chlorotrityl resin for peptide **2** (Fig. 1) employing Fmoc chemistry and the TBTU/DIPEA coupling strategy. We envisioned a synthetic route in which all steps would be done while the peptide was still attached to the solid support (Scheme 1), which would minimize losses from handling and successive preparative HPLC purifications. In this reaction sequence, coupling of Boc-HYNIC was done by TBTU/DIPEA coupling strategy after chain assembly by standard Fmoc-based SPPS. The cyclization was also done in solid phase by I_2 oxidation method. When the peptide chain was completely assembled, the Fmoc-protecting group was removed, and cleavage/deprotection was carried out using TFA-containing water, with EDT and TIS as scavengers. Acid-labile side chain-protecting groups were utilized so that simultaneous side chain deprotection and cleavage of the peptide could be achieved. The peptides **1** and **2** were purified by HPLC on a C_{18} reverse-phase column (gradient elution with CH_3CN/H_2O). After lyophilization, they were obtained as white powders, in yields ranging from 44 to 60 %. The purity of all conjugates was determined to be >95 % on the basis of absorption at 254 nm. A typical HPLC-chromatogram of **1** is shown (Supplementary Material, Fig. S1).

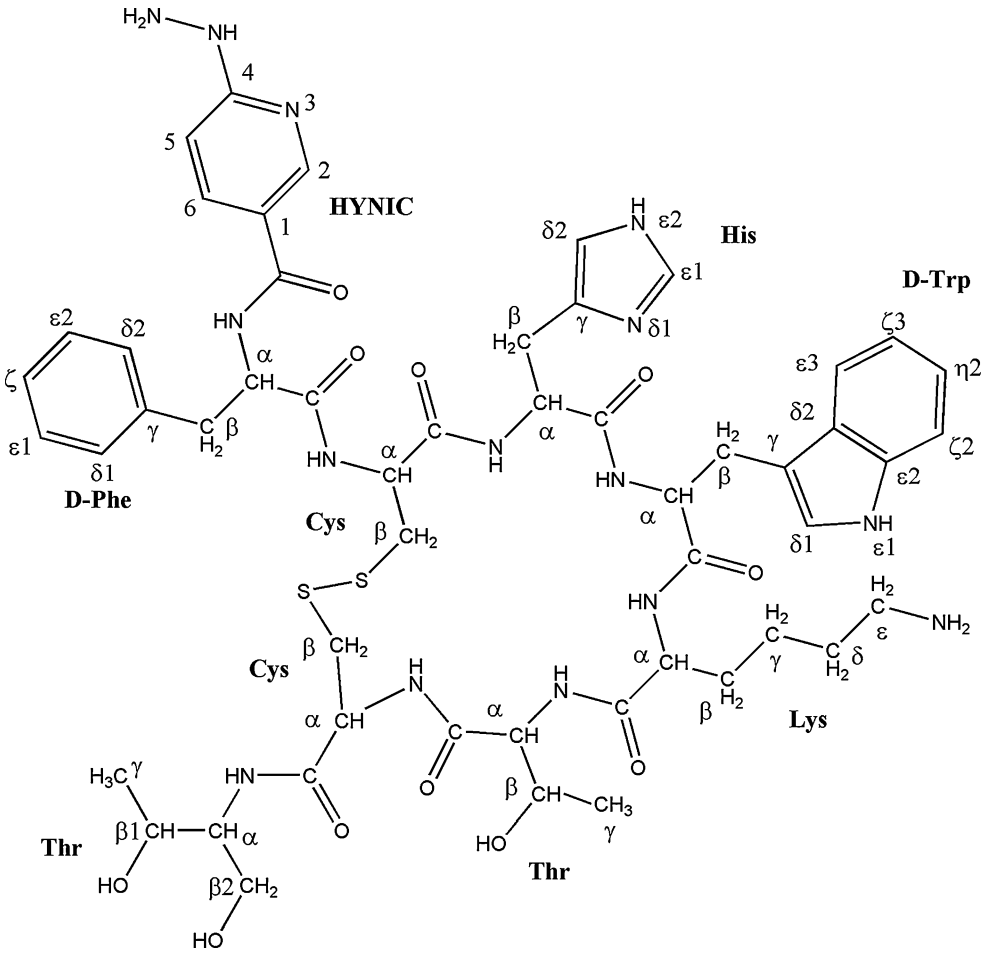

Fig. 1 Depiction of residue naming and atom numbering for the conjugate HYNIC-His[3]-Octreotate (**1**)

For all the conjugates, formation of the desired product was confirmed by MALDI-TOF MS at high resolution (Supplementary Material, Fig. S2). Ellman's test confirmed that the free thiol group was absent in the peptides **1** and **2** obtained after deblocking with cocktail. Also from the NMR data, the formation of S–S bond was confirmed. The random coil chemical shift values of C_α and C_β are 55.3 and 40.5 for Cys_{oxd} but 58.2 and 29.4 for Cys_{red}. We observed the values to be 55.3 and 40.5, agreeing with Cys_{oxd} value of random coil, which confirms the formation of S–S bond (Supplementary Material, Table S1). The IR absorption bands were characteristic of amino (3,280 cm^{-1}) and amide carbonyl (1,664 cm^{-1}) groups (Supplementary Material, Fig. S3). Amino acid analysis of **1** showed it to consist of D-phe, Cys × 2, Thr × 2, Lys, D-Trp and His by HPLC. The ^{1}H NMR spectrum of **1** in D_2O showed peaks for two methyl groups of two threonine residues (δ 1.15, 1.19), nine $-CH_2$ groups (δ 0.36, 0.52, 1.28, 1.31, 1.61–1.65, 2.64–2.73, 2.83–2.88, 2.98–3.03, 3.17–3.21, 3.28–3.32), fifteen aromatic –CH protons (δ 8.48, 8.26, 8.03, 7.63, 7.51, 7.35–7.38, 7.28–7.31, 7.25, 7.22, 7.17, 6.98) and ten proton resonances (δ 5.11, 4.99, 4.86–4.89, 4.74, 4.56, 4.38, 4.32, 4.24–4.27, 3.95), which were indicative of α-protons of amino acid residues. The presence of seven-quaternary carbon and nine carbonyl carbons were indicated by the ^{13}C NMR spectra. Assignment of ^{1}H NMR signals to specific nuclei in individual residues was done by COSY, HSQC and HMBC experiments to show the complete spin systems of the amino acid residues (Supplementary Material, Table I; Figs. S4, S5). The carbonyl signal at 167.2 was assigned to amide carbonyl carbon of the HYNIC residue, which was confirmed by HMBC cross peaks for this carbon with both H6 (δ 8.03) and H2 (δ 8.26) of HYNIC residue. Similarly, another carbonyl signal at δ 175.9 showed HMBC correlations with Hα proton of threonine (8th) residue. While most chemical shifts fall in the range normally expected, the Lys[5] γH_2 and δH_2 resonances are highly upfield, most probably due to shielding by ring current from Trp[4] (Supplementary Material, Figs. S7–S18).

Structural study by circular dichroism

Far-ultraviolet circular dichroism (CD) spectroscopy is a widely used tool to investigate peptide and protein secondary structure. Below 250 nm, CD spectra of peptides

are dominated by the amide chromophore of the chiral peptide backbone (Kelly and Price 2000). For many studies, trifluoroethanol (TFE) has been used as a structure-inducing cosolvent that can promote and strengthen intramolecular hydrogen bonding and thereby increase the order in peptides that are otherwise unstructured in aqueous solution (Rodziewicz-Motowidio et al. 2002; Kelly and Price 2000). The secondary peptide conformation, determined by the Jasco software, was found to contain ~3.2 % α-helix, ~51.8 % β-sheet and ~45.1 % random coil conformation for HYNIC-His^3-TATE, but ~60.9 % β-sheet and ~39.1 % random coil conformation for HYNIC-TOC in water. Upon addition of equal volume of TFE, dramatic changes were noted. We observed decrease in randomness (from 39.1 to 30.7 % for HYNIC-TOC and from 45.1 to 34.0 % for HYNIC-His^3-TATE) and α-helix (from 3.2 to 0 % for HYNIC-His^3-TATE) but increase in β-sheet (from 60.9 to 69.3 % for HYNIC-TOC and from 51.8 to 66.0 % for HYNIC-His^3-TATE) conformation. HYNIC-His^3-TATE showed a strong positive band at ~194 nm along with a strong negative band at ~200 nm and a weak negative band at ~217 nm, which are consistent with a mixture of α-helix, β-sheet, and random coil conformational elements. But after addition of equal volume of TFE, we observed only a strong negative band at ~204 nm and weak negative band at ~219 nm. HYNIC-TOC showed negative bands at ~198 and ~219 nm along with a weak positive band at ~230 nm, consistent with a mixture of β-sheet, and random coil conformational elements. But after addition of equal volume of TFE, we observed a negative band at ~205 nm and a weak broad negative band at ~215 nm along with a positive band at ~232 nm (Fig. 2).

Radiolabeling and quality control

Radiochemical purity of complex **3** was estimated chromatographically using ITLC-SG. Also the radiochemical purity of radiolabeled peptide was validated by RP-HPLC. The labeling yield was found to be more than 98 % by ITLC. We obtained high radiochemical yield (98.49 ± 0.3 %, $n = 5$) with very low amount of ^{99m}Tc-pertechnetate (0.1 ± 0.04 %, $n = 5$), ^{99m}Tc-radiocolloid (0.5 ± 0.06 %, $n = 5$) and ^{99m}Tc-coligand (1.0 ± 0.03 %, $n = 5$). In RP-HPLC analysis of complex **3**, we observed a single major peak at 12.745 min (elution time) with minor impurities (Fig. 3). In ITLC with 2-Butanone solvent, the labeled complex **3**, ^{99m}Tc-coligands and ^{99m}Tc-colloid remained at the origin ($R_f = 0$) while $^{99m}TcO_4^-$ moved to the solvent front ($R_f = 1$). With 0.1 M sodium citrate, pH

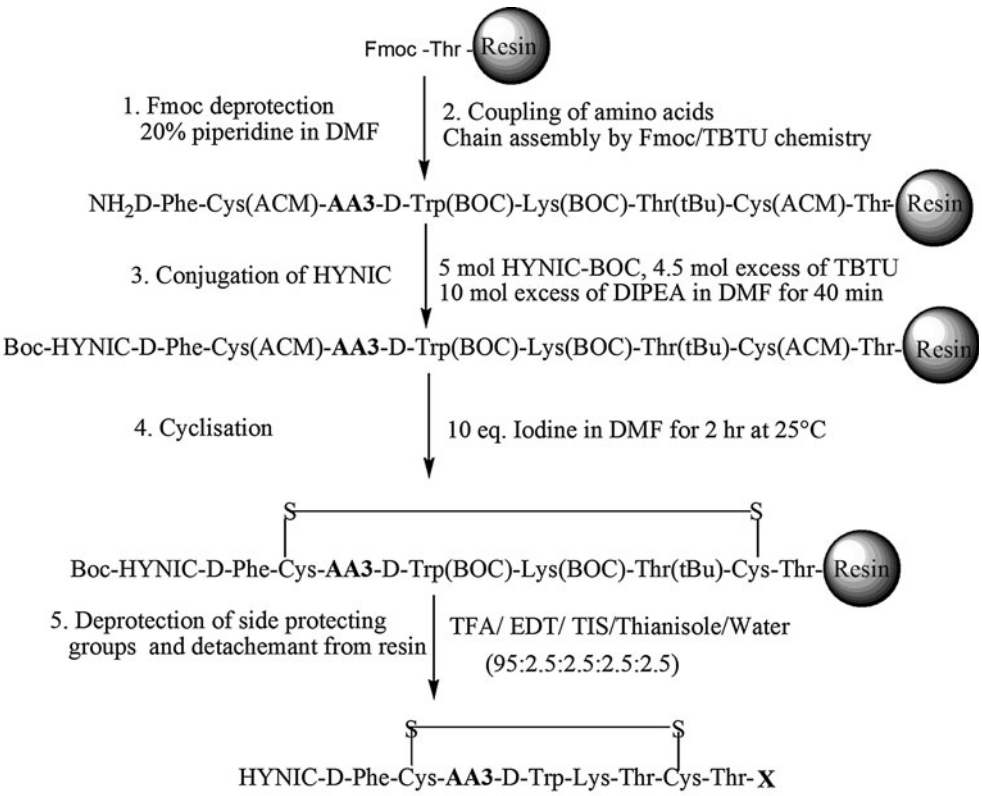

Scheme 1 Synthesis of HYNIC-His^3-Octreotate (**1**) and HYNIC-TOC (**2**)

HYNIC-His^3-octreotate **(1); AA3** = His^3 and **X** = COOH
HYNIC-TOC **(2); AA3** = Tyr^3 and **X** = CH_2OH

5.1 solvent system, the labeled complex **3** and ^{99m}Tc-colloid remained at the origin ($R_f = 0$) but ^{99m}Tc-coligands and $^{99m}TcO_4^-$ moved to the solvent front ($R_f = 1$). Using methanol/1 M ammonium acetate (1:1) solvent system, ^{99m}Tc-colloid remained at the origin ($R_f = 0$) and the labeled complex **3**, ^{99m}Tc-coligands and $^{99m}TcO_4^-$ moved to the solvent front ($R_f = 1$).

In vitro serum stability study

From the stability study, we found that complex **3** was stable in PBS (pH = 7.4), serum and aqueous solutions for 24 h post-labeling at room temperature. This was assessed by ITLC method at different time intervals of 1, 2, 4, 6, 8, 12 and 24 h at room temperature. Also the stability of radiolabeled peptides was validated by RP-HPLC using gradient II as solvent system at different time intervals (Supplementary Material, Fig. S6).

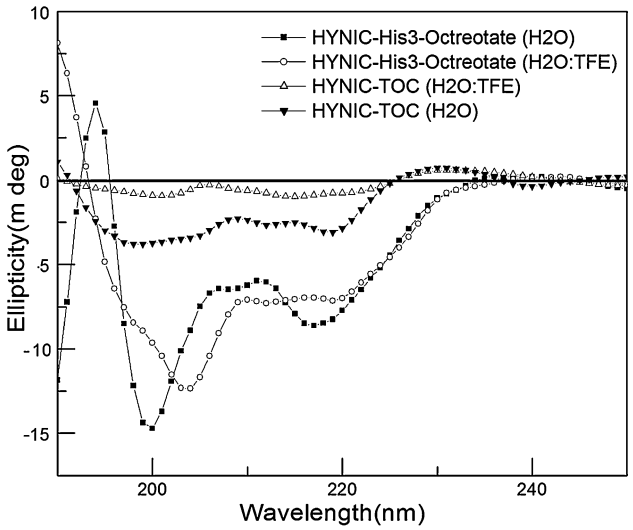

Fig. 2 CD spectra of HYNIC-His^3-Octreotate and HYNIC-TOC in pure water (*solid symbol*) and TFE:H_2O (1:1), respectively. Spectra were recorded with 865 μM solutions and are normalized

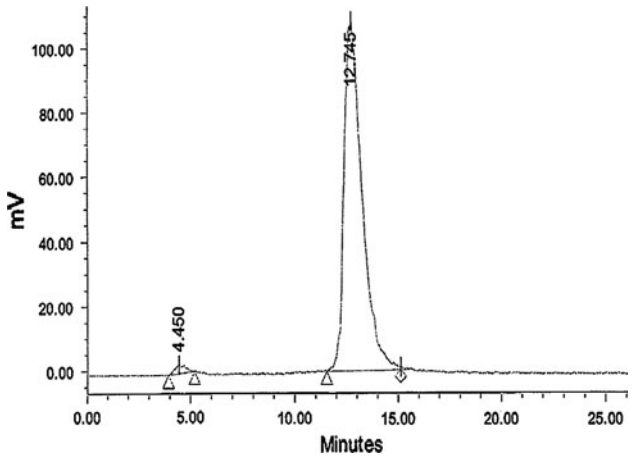

Fig. 3 RP-HPLC analytical chromatogram of radiopeptide complex ^{99m}Tc-HYNIC-His^3-Octreotate; purity by HPLC: 98.3 %. R_t = 12.745 min; conditions: C_{18} column, solvent A = 0.1 % TFA (v/v) in water, solvent B = 0.085 % TFA (v/v) in acetonitrile; elution with a linear gradient of 10–90 % solvent B in solvent A over 45 min following gradient system II

Metabolic stability in rat kidney and urine

Results of metabolism studies indicate that the radiopeptide was stable to enzymatic changes. The retention peaks obtained from the HPLC analysis of kidney and urine samples collected after 120 min of bolus injection of ^{99m}Tc-peptide was similar to the R_t value of complex **3** by RP-HPLC using gradient II as solvent system. This result demonstrates again the high in vivo stability of the complex (Supplementary Material, Fig. S7).

Radioligand internalization

The internalization property of complex **3** (^{99m}Tc-HYNIC-His^3-Octreotate) was studied in C6 glioma cells over time. The cells were incubated at 37 °C with the radioligand with or without the addition of a large excess of cold peptides **1** and **2** (non-specific series). Radioactivity bound to the receptor on the membrane was "acid washed" with glycine buffer of pH 2.8 to determine the membrane-bound activity, whereas radioactivity in the cell (internalized activity) was collected after lysing the cells by treatment with 1 N NaOH. The curve of percent internalized activity versus the selected time points was drawn, showing the result in respect of the time-dependent and specific internalization of the radioligand into C6 glioma cells. During 30 min, the radioligand showed 65.45 ± 0.56 % specific cell uptake, which increased to 75.39 ± 0.61 % at 2 h. In all experiments, internalization was strongly reduced in the presence of excess cold peptides **1** and **2**. During 30 min, the internalization was strongly reduced to 24.75 ± 0.38 % from 65.45 ± 0.56 % and, at 4 h, internalization was strongly reduced to 12.25 ± 0.47 % from 68.52 ± 0.23 % in the presence of excess cold peptides **1** and **2** (Fig. 4).

In vitro receptor binding assays

Radiopeptide **3** (^{99m}Tc-HYNIC-His^3-Octreotate) was displaced from somatostatin binding sites in rat brain cortex sections in a monophasic and dose-dependent manner by compounds **1** and **2**. The IC_{50} value was found to be 21 and 2.87 nM for radiopeptide complexes **3** (^{99m}Tc-HYNIC-His^3-Octreotate) and **4** (^{99m}Tc-HYNIC-TOC), respectively. Representative displacement curves for radiopeptides **3** and **4** are shown in Fig. 5.

Biodistribution in normal rats

Biodistribution results of radiopeptide **3** were obtained from Sprague-Dawley rats administered intravenously and sacrificed at 2, 15, 60, 120 min post-administration. The results are expressed as the percentage of the injected dose/gram of organ (% ID/g). Soon after administration, radiopeptide **3** was rapidly cleared from the blood and body of rat into the urine via the kidney and urinary tract as a result of its high hydrophilicity. Results showed higher uptake in kidney than any other organ and this gradually decreased as time passed. The kidney uptake (% ID/g) was 3.87 ± 0.12, 3.79 ± 0.14, 3.52 ± 0.01 and 2.46 ± 0.01 at 2, 10, 30, 60 min post-administration. Blood clearance was faster with rapid excretion through kidneys. This indicates that kidney and urinary system represents the predominant excretion route for radiopeptide complex **3**. There was relatively low uptake in liver for complex **3** but complex **4** showed some uptake. Quite low uptake was observed in stomach (0.11 ± 0.03, 0.09 ± 0.01, 0.07 ± 0.01, 0.05 ± 0.01) and intestine (0.08 ± 0.001, 0.05 ± 0.002, 0.02 ± 0.006, 0.01 ± 0.003) at all the time points, indicating minimal in vivo decomposition of the chelate to form free $^{99m}TcO_4$/$^{99m}TcO_2$. The results of scintigraphy imaging studies and renogram study also showed the highest uptake in the kidney which gradually decreased as time passed (Fig. S8, Fig. 6).

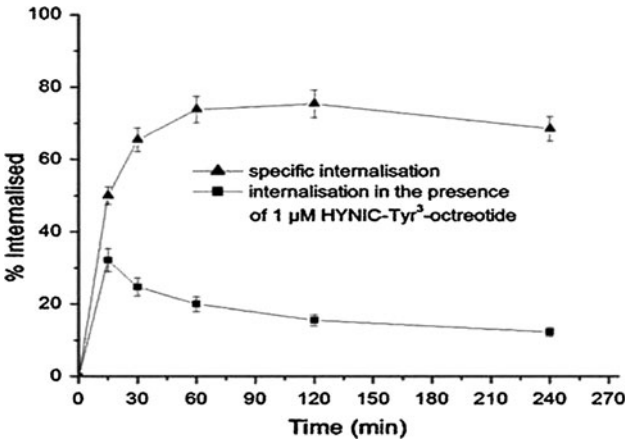

Fig. 4 Time course of the internalization of ^{99m}Tc-HYNIC-His^3-Octreotate in C6 glioma cells at 37 °C. The internalization percentage was determined by dividing acid-resistant binding by total specific binding. Data represent the mean values of three independent experiments

Tumor uptake of ^{99m}Tc-HYNIC-His^3-Octreotate

Tissue distribution data for ^{99m}Tc-HYNIC-His^3-Octreotate in Lewis rats bearing SSTr-positive C6 glioma tumors are given as % ID/g in Table 1. High radioactivity accumulation was evident in SSTR-positive organs tested, including the pancreas, stomach and intestines. This uptake represented mostly specific interaction with SSTRs as co-injection of 100 μg of excess cold peptide reduced the uptake in these organs very significantly ($p < 0.005$) as compared to control values. Similarly, high uptake was observed in the C6 glioma tumors at 45 min p.i. The tumor values increased significantly between 10 min (0.91 ± 0.23 % ID/g) and 45 min (1.27 ± 0.15 % ID/g) p.i. By co-injection of excess of cold complex, uptake in the C6 glioma tumors was reduced very significantly (by >90 %), suggesting again a receptor-mediated process. ^{99m}Tc-HYNIC-His^3-Octreotate was cleared very rapidly from the blood and was excreted from the body of rat predominantly via the kidneys into urine, showing a small percentage of hepatobiliary excretion. Urine collected 30 min after injection of ^{99m}Tc-HYNIC-His^3-Octreotate in

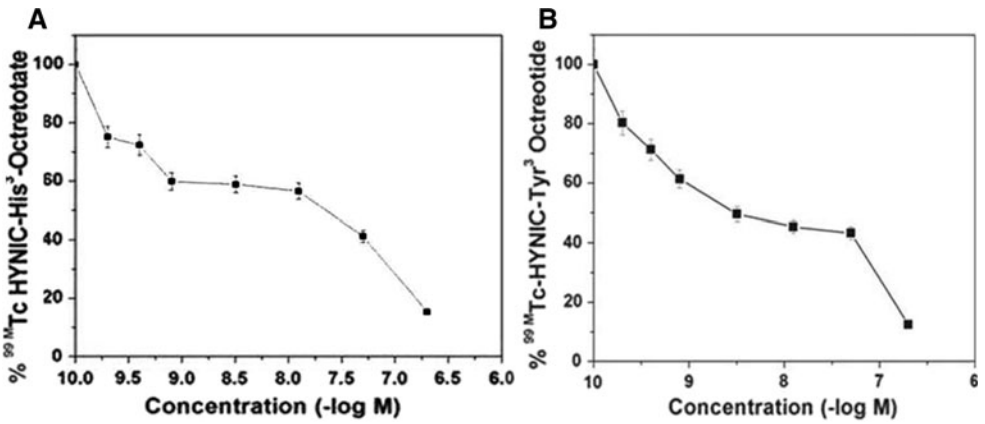

Fig. 5 **a** Competitive inhibition specific binding HYNIC-TOC to rat brain cortex preparations by ^{99m}Tc-HYNIC-His^3-Octreotate; *each point* represents mean of three individual determinations, IC_{50} concentrations were determined. **b** Competitive inhibition specific binding HYNIC-TOC to rat brain cortex preparations by ^{99m}Tc-HYNIC-Tyr^3-Octreotide; *each point* represents mean of three individual determinations, IC_{50} concentrations were determined

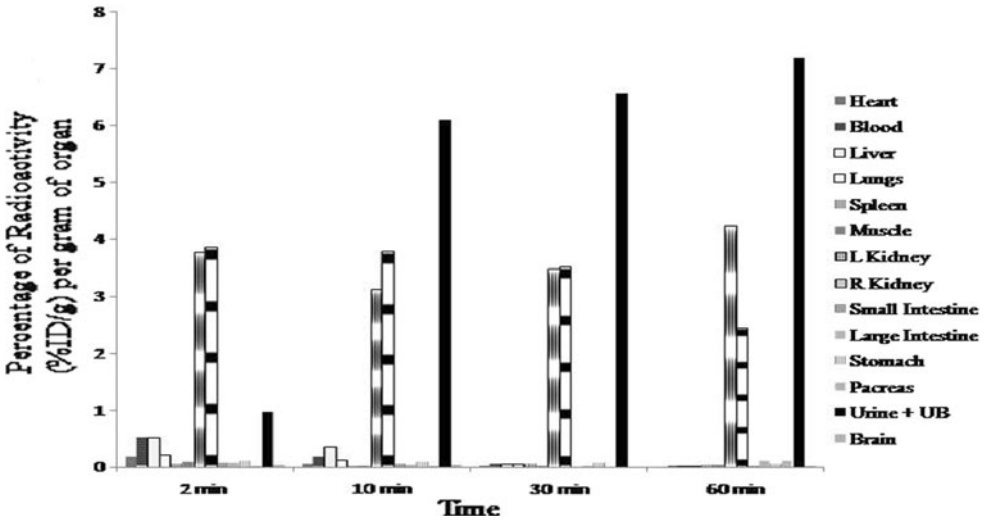

Fig. 6 Organ biodistribution (% ID/g) of complex ^{99m}Tc-HYNIC-His^3-Octreotate (200 µl) in normal rats ($n = 8$)

Table 1 Biodistribution data (% ID/g, mean ± SD) of ^{99m}Tc-HYNIC-His^3-Octreotate in C6 glioma tumor-bearing Lewis rats at 10 and 45 min pi ($n = 4$)

Organs	10 min	45 min	45 min blocked
Heart	1.8 ± 0.43	1.2 ± 0.23	0.9 ± 0.27
Blood	1.25 ± 0.33	0.73 ± 0.13	0.33 ± 0.23
Liver	1.6 ± 0.06	0.72 ± 0.08	0.28 ± 0.11
Lungs	3.01 ± 0.21	1.22 ± 0.18	0.83 ± 0.35
Spleen	0.12 ± 0.03	0.11 ± 0.01	0.04 ± 0.01
Muscle	0.19 ± 0.02	0.15 ± 0.01	0.11 ± 0.04
Kidney	2.86 ± 0.17	1.71 ± 0.11	0.91 ± 0.33
S. intestine	0.84 ± 0.04	0.52 ± 0.03	0.32 ± 0.07
L. intestine	0.85 ± 0.07	0.47 ± 0.05	0.25 ± 0.02
Stomach	0.95 ± 0.13	0.79 ± 0.07	0.33 ± 0.13
Urine	1.4 ± 0.23	4.02 ± 0.15	2.11 ± 0.12
Pancreas	2.71 ± 0.33	1.71 ± 0.03	0.53 ± 0.23
Brain	0.1 ± 0.01	0.07 ± 0.03	0.03 ± 0.01
Tumor	0.91 ± 0.23	1.27 ± 0.15	0.35 ± 0.03
Tumor to normal tissue ratios			
Tumor/blood	0.73	1.74	
Tumor/liver	0.43	1.76	
Tumor/kidneys	0.32	0.75	
Tumor/muscle	4.81	8.47	
Tumor/intestine	1.07	2.71	
Tumor/stomach	0.96	1.61	
Tumor/pancreas	0.34	0.74	

Non-specific uptake was determined by co-injection of 100 µg cold HYNIC-TOC (blocked animals)

healthy rats was found to contain the major excreted portion. Radiochemical analysis of such urine samples showed that ^{99m}Tc-HYNIC-His^3-Octreotate was cleared into the urine as intact peptide. Due to the rapid clearance of ^{99m}Tc-HYNIC-His^3-Octreotate from non-target tissues, high tumor to background ratios were easily achieved, illustrating its suitability for targeted tumor imaging.

Imaging

Static images of scintigraphy and renogram curves of rats bearing C6 glioma tumors in the femur area and of normal rat are presented in Fig. 7. Scintigraphy showed high specific uptake in the pancreas and tumor after 45 min. As shown by the planar images, excellent clearing properties of ^{99m}Tc-HYNIC-His^3-Octreotate are evident in both animals. Administration of excess unlabeled cold peptide (100 µg HYNIC-TOC) to a control animal reduced the uptake in receptor-positive organs and the tumor. After 45 min, because of background clearance, the tumor to normal organ ratio improved in the non-blocked animals.

Discussion

In the course of this work, we understood synthesis and biological evaluation of a novel ^{99m}Tc-based somatostatin analog **3** with potential use in the visualization of SSTR-positive tumors. Though several somatostatin analogs labeled with a wide spectrum of radionuclides have already been reported (Lewis et al. 1999; Bakker et al. 1991) and an established radiopharmaceutical [^{111}In] OctreoScan is available (Krenning et al. 1992; de Jong et al. 1998), the search for a ^{99m}Tc-somatostatin radiotracer has intensified (Bangard et al. 2000; Thakur et al. 1997; Weiner and Thakur 2002) due to the superior nuclear properties of ^{99m}Tc and its cost effectiveness (Liu et al. 1997; Liu and Edwards 1999). Previous efforts to develop such an agent have mainly utilized octreotide/[Tyr^3] octreotide as the SSTR recognition site. A variety of chelators attached to the N-terminal of the octapeptide and serving as the

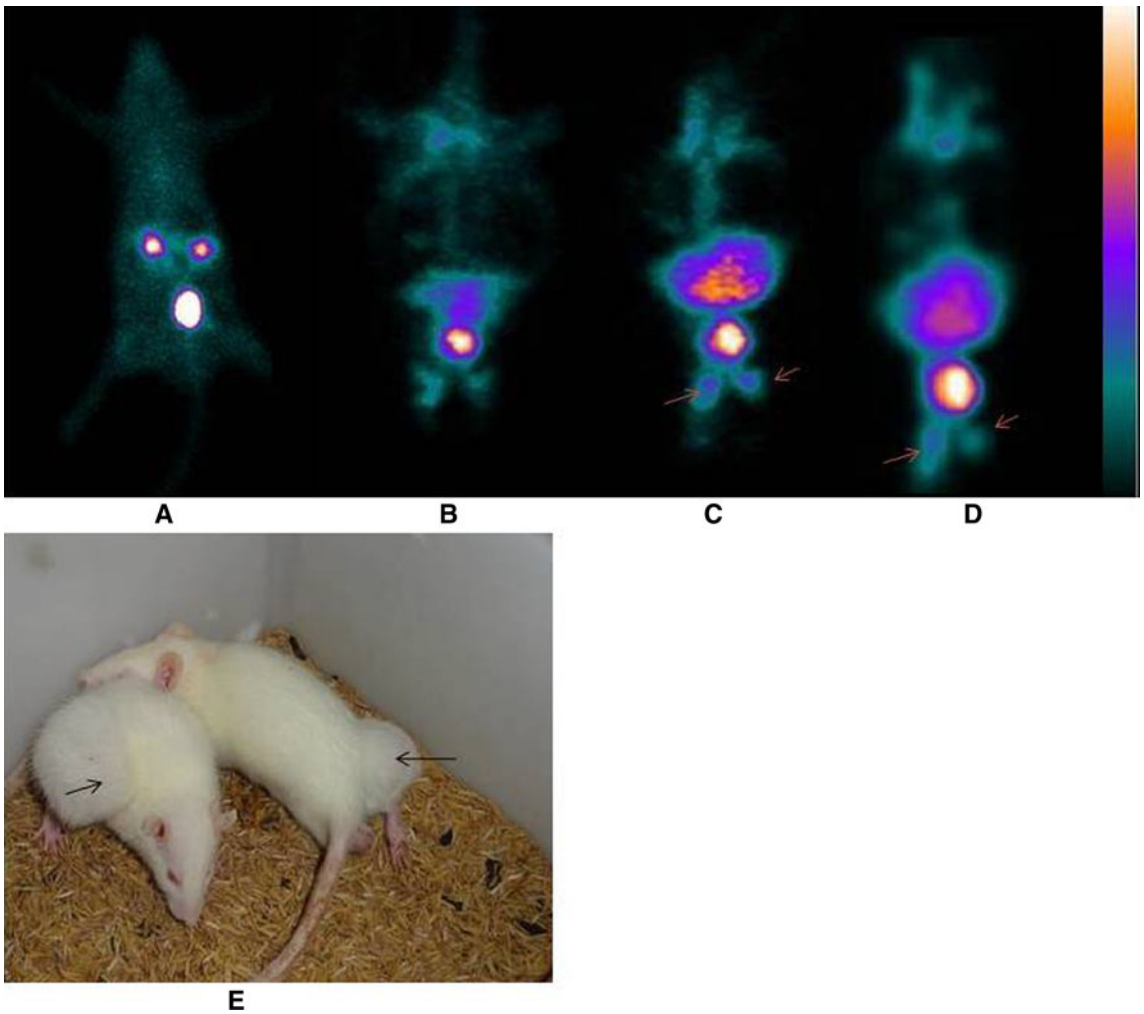

Fig. 7 **a** Planar static images of normal rat at 45 min after i.v. injection of ^{99m}Tc-HYNIC-His^3-Octreotate (20 MBq). **b** SPECT image on C6 glioma tumor-bearing rat showing blocking (100 μg of cold HYNIC-TOC) of ^{99m}Tc-HYNIC-His^3-Octreotate uptake in receptor-positive organs and tumor. **c** SPECT image on C6 glioma tumor-bearing rat at 10 min showing uptake in receptor-positive organs and tumor. **d** SPECT image on C6 glioma tumor-bearing rat at 45 min showing uptake in receptor-positive organs and tumor. **e** Tumor developed in rats after 20 days of subcutaneous injection of 10^7 C6 glioma cell into flank of 6-week-old male Lewis rat

radiometal-binding site have been tested. Peptide modifications using HYNIC have so far given the best results in terms of tissue distribution profiles and tumor-targeting properties (Bangard et al. 2000).

The present work, which is a continuation of our previous work (Behera et al. 2011), has shown that [Tyr^3] octreotide is the peptide of choice. Substitution of Phe^3 by Tyr^3 and of Thr (ol)^8 by Thr^8 in the original octreotide motif was expected to increase the hydrophilicity and improve the in vivo performance of the final ^{99m}Tc radioligand. Similarly, we have substituted Tyr^3 by His^3 and Thr (ol)^8 by Thr^8 in the Tyr^3 octreotide motif for the same purpose. The improved kidney clearance of ^{99m}Tc-HYNIC-His^3-Octreotate is most likely caused by the free carboxylate group, which is a known structural feature that enables rapid handling of carboxylic acid derivatives in the kidney. Interestingly, the two radiolabeled peptides are also handled similarly by endopeptidases in rat. They were excreted essentially unchanged into the urine after 2 h. This shows the high in vivo stability of these compounds.

With the aim to prepare a ^{99m}Tc-labeled analog that is at least comparable with ^{111}In-DTPA-octreotide in its ability to image SSTRs in vivo, we took up the preparation of a ^{99m}Tc tracer with good in vitro and in vivo stability, high affinity for SSTRs, and a favorable pattern of biodistribution. This last parameter required that the compound undergoes rapid blood clearance while having low uptake in receptor-negative tissues and organs of excretion. In particular, the radiopharmaceutical should be excreted predominantly through the renal system to avoid accumulation in the gastrointestinal tract. This was indeed confirmed by renogram and SPECT analysis study of our product.

In our study HYNIC was conjugated with Tyr^3 octreotide and His^3-Octreotate before cleavage of peptide from resin and its subsequent cyclization in solid phase. From the analytical data (MALDI mass, NMR, IR and HPLC), we could characterize the compound well and found it to be of high purity (Supplementary Material, Figs. S9–S20). Structural study by circular dichroism revealed that our HYNIC-conjugated peptides possess strong secondary structural features like β-sheet and random coil conformations. After the addition of equal volume of TFE, proportion of β-sheet conformation increased and that of random coil conformation decreased, in accordance with the literature reports (Grace et al. 2008; Melacini et al. 1997) that β-sheet conformation is needed for octreotide analogs for binding to SSTr. Bands at $\sim$204, $\sim$205 nm are indicative of α-turn conformation (Gardiner et al. 2008). Labeling with ^{99m}Tc was accomplished by Tricine/EDDA exchange method simply by mixing tin chloride in Tricine/EDDA at pH 6.8–7.2 and briefly incubating this mixture at 90 °C for 15 min. The results from ITLC and HPLC data showed that the labeling procedure was simpler and high yielding and insured high radiochemical purity for the complexes. In our method of labeling, the easy formation of complexes **3** and **4** does away with purification of the reaction mixture by column chromatography, and the stability of the product in the open vial for at least 24 h following labeling presents clear practical advantages for future routine application in a clinical environment. Incorporation of the radiometal by the bidentate ligand was practically quantitative, leading to a single radioactive species, **3** showing high kinetic stability and hydrophilicity. As demonstrated by in vitro and in vivo tests following labeling, ^{99m}Tc-HYNIC-His^3-Octreotate retained its receptor affinity. These results strongly suggest that the disulfide bridge of the octapeptide remained unaffected under the reduction conditions of the labeling process. The resistance of complex **3** to enzymatic degradation in plasma and the fact that it is excreted intact into the urine reflect its stability.

The affinity binding of complex **3** was found to be in the nanomolar range (IC_{50} = 21 nM), and it showed a moderate and receptor-specific internalization into C6 glioma cells compared to standard (IC_{50} = 2.87 nM). These data show that radioligands have the potential to target tumors with SSTr expression, either alone or concomitantly with other subtypes. C6 glioma cell line mostly over expresses SSTr 2, SSTr 3, and SSTr 5 (Barbieri et al. 2008). Although SSTR 2 is probably the most abundantly expressed SRIF receptor in human cancer (Vaidyanathan et al. 2003; Reubi et al. 2001; Wild et al. 2003), subtypes SSTR 1, SSTR 3, SSTR 4 and SSTR 5 may also be of interest. Storch et al. (2005) reported that complex **4** has more affinity for SSTR 2 binding compare to SSTR 3 and SSTR 5. Decristoforo et al. (2000a) also found an IC_{50} of 0.65 nM for complex **4** in AR42J cell line, which predominantly expresses the SSTR 2 receptor only. But in our study we found the IC_{50} of 2.87 nM for complex **4** and 21 nM for the new complex **3** in C6 glioma cell line, which expresses not only SSTR 2 but also SSTR 3 and SSTR 5. The difference in the results may be due to the use of different methodologies for binding study and of cell lines that express different receptors.

In internalization study, the peptide showed rapid internalization into C6 glioma cells. Our data showed that complex **3** has a higher potential to bind and internalize in tumor cells with SSTr expression. During 30 min, the radioligand showed 65.45 ± 0.56 % non-specific cell uptake, which increased to 75.39 ± 0.61 % at 2 h. A study of the efflux of radioligand from C6 glioma cells revealed that 68.52 ± 0.23 % activity was retained in the cells after 4 h. We found a close approximation to a steady state after 4 h of internalization of the radioligand, which could mean that the activity remaining in the cell is simply trapped (Vaidyanathan et al. 2003). This order follows the receptor affinity of the radiopeptides, indicating that receptor affinity is the major factor determining the rate of internalization. The results of blocking experiment showed that these uptakes were specific and receptor mediated. The accumulation of ^{99m}Tc-HYNIC-His^3-Octreotate in rats with C6 glioma tumor was receptor mediated by the blocking of SSTr-positive C6 glioma tumors and was >90 % in all SSTR-positive organs by co-administration of an excess of cold octreotide.

The scintigraphy of the tumor-bearing Lewis rats on gamma-camera showed specific uptake in the tumor and the SSTR-positive organs after 45 min. Mostly, the tumor and all receptor-positive organs were blocked by the addition of an excess cold octreotide at 45 min. Because of background clearance, the tumor to normal ratio improved. Therefore, this radioligand may be used further for clinical trials to be developed as a radiopharmaceutical.

Conclusion

We have successfully developed a new HYNIC-based peptide for diagnostic application. The new somatostatin analog HYNIC-His^3-Octreotate was successfully synthesized, characterized and radiochemically and biologically evaluated. The new derivative has the potentiality for SSTR imaging in SSTR-positive tumors. This report warrants more study to develop ^{99m}Tc-HYNIC-His^3-Octreotate as a tracer for radiopharmaceutical.

Acknowledgments The authors gratefully acknowledge Prof. Siddhartha Roy Director, Indian Institute of Chemical Biology

(IICB), Kolkata, India and Dr. N. Sivaprasad, Sr. General Manager, Board of Radiation and Isotope Technology (BRIT), Navi Mumbai, India for their support. Also thanks to Dr. Basudeb Achari for valuable suggestions, Dr. Krishna Das Saha, for Tissue culture hood facility, Dr. Maidul Hussain and Dr. G. Suresh kumar for CD spectroscopy facility of Indian Institute of Chemical Biology (IICB), Kolkata, India. We also thank Board of Research in Nuclear Sciences (BRNS), Department of Atomic Energy (DAE) and Council of scientific and industrial research (CSIR) for financial support.

References

Abrams MJ, Juweid M, Tenkate CI, Schwartz DA, Hauser MM, Gaul FE, Fuccello AJ, Rubin RH, Strauss HW, Fischman AJ (1990) Technetium-99m-human polyclonal igG radiolabeled via the hydrazino nicotinamide derivative for imaging focal sites of infection in rats. J Nucl Med 31(12):2022–2028

Bakker WH, Albert R, Bruns C, Breeman WAP, Hofland LJ, Marbach P, Pless J, Pralet D, Stolz B, Koper JW, Lamberts SWJ, Visser TJ, Krenning EP (1991) In-111-DTPA-D-Phe^{1}-octreotide, a potential radiopharmaceutical for imaging of somatostatin receptor-positive tumors-synthesis, radiolabeling and invitro validation. Life Sci 49(22):1583–1591

Bangard M, Behe M, Guhlke S, Otte R, Bender H, Maecke HR, Biersack HJ (2000) Detection of somatostatin receptor-positive tumours using the new Tc-99m-tricine-HYNIC-D-Phe(1)-Tyr(3)-octreotide: first results in patients and comparison with In-111-DTPA-D-Phe(1)-octreotide. Eur J Nucl Med 27(6):628–637

Barbieri F, Pattarozzi A, Gatti M, Porcile C, Bajetto A, Ferrari A, Culler MD, Florio T (2008) Somatostatin receptors 1, 2, and 5 cooperate in the somatostatin inhibition of C6 glioma cell proliferation in vitro via a phosphotyrosine phosphatase-eta-dependent inhibition of extracellularly regulated kinase 1/2. Endocrinology 149(9):4736–4746

Behera A, De K, Chandra S, Chattopadhyay S, Misra M (2011) Synthesis, radiolabelling and biodistribution of HYNIC-Tyr^{3} octreotide: a somatostatin receptor positive tumour imaging agent. J Radioanal Nucl Chem 290(1):123–129

Berges JA, Fisher AE, Harrison PJ (1993) A comparison of Lowry, Bradford and Smith protein assays using different protein standards and protein isolated from the marine diatom *Thalassiosira pseudonana*. Mar Biol 115(2):187–193

Breeman WAP, de Jong M, Kwekkeboom DJ, Valkema R, Bakker WH, Kooij PPM, Visser TJ, Krenning EP (2001) Somatostatin receptor-mediated imaging and therapy: basic science, current knowledge, limitations and future perspectives. Eur J Nucl Med 28(9):1421–1429

De Jong M, Breeman WAP, Bakker WH, Kooij PPM, Bernard BF, Hofland LJ, Visser TJ, Srinivasan A, Schmidt MA, Erion JL, Bugaj JE, Macke HR, Krenning EP (1998) Comparison of In-111-labeled somatostatin analogues for tumor scintigraphy and radionuclide therapy. Cancer Res 58(3):437–441

Decristoforo C, Melendez-Alafort L, Sosabowski JK, Mather SJ (2000) ^{99m}Tc-HYNIC-[Tyr3]-octreotide for imaging somatostatin-receptor-positive tumors: preclinical evaluation and comparison with ^{111}In-octreotide. J Nucl Med 41(6):1114–1119

Fischman AJ, Babich JW, Strauss HW (1993) A ticket to ride: peptide radiopharmaceuticals. J Nucl Med 34(12):2253–2263

Gabriel M, Decristoforo C, Maina T, Nock B, von Guggenberg E, Cordopatis P, Moncayo R (2004) 99mTc-N4-[Tyr3]Octreotate Versus 99mTc-EDDA/HYNIC-[Tyr3]Octreotide: an intrapatient comparison of two novel Technetium-99m labeled tracers for somatostatin receptor scintigraphy. Cancer Biother Radiopharm 19(1):73–79. doi:10.1089/108497804773391702

Gandomkar M, Najafi R, Shafiei M, Mazidi M, Ebrahimi SES (2007) Preclinical evaluation of Tc-99m/EDDA/tricine/HYNIC0, 1-Nal(3), Thr(8)-octreotide as a new analogue in the detection of somatostatin-receptor-positive tumors. Nucl Med Biol 34(6):651–657. doi:10.1016/j.nucmedbio.2007.06.006

Gardiner J, Langenegger D, Hoyer D, Beck AK, Mathad RI, Seebach D (2008) The enantiomer of octreotate binds to all five somatostatin receptors with almost equal micromolar affinity—a comparison with SANDOSTATIN. Chem Biodivers 5(7):1213–1224. doi:10.1002/cbdv.200890110

Grace CRR, Erchegyi J, Samant M, Cescato R, Piccand V, Riek R, Reubi JC, Rivier JE (2008) Ring size in octreotide amide modulates differently agonist versus antagonist binding affinity and selectivity. J Med Chem 51(9):2676–2681. doi:10.1021/jm701445q

Kelly SM, Price NC (2000) The use of circular dichroism in the investigation of protein structure and function. Curr Protein Pept Sci 1(4):349–384. doi:10.2174/1389203003381315

Koenig JA, Kaur R, Edwardson JM, Humphrey PPA (1996) Somatostatin receptors in Neuro2A neuroblastoma cells: pharmacological characterisation and internalisation of I-125-BIM-23027, a somatostatin analogue. Br J Pharmacol 118:P26

Koenig JA, Edwardson JM, Humphrey PPA (1997) Somatostatin receptors in Neuro2A neuroblastoma cells: operational characteristics. Br J Pharmacol 120(1):45–51

Krenning EP, Bakker WH, Kooij PPM, Breeman WAP, Oei HY, Dejong M, Reubi JC, Visser TJ, Bruns C, Kwekkeboom DJ, Reijs AEM, Vanhagen PM, Koper JW, Lamberts SWJ (1992) Somatostatin receptor scintigraphy with Indium-111-DTPA-D-Phe-1-octreotide in man: metabolism, dosimetry and comparison with Iodine-123-Tyr-3-octreotide. J Nucl Med 33(5):652–658

Lee TW, Chang SR, Chen ST, Tsai ZT (1998) Convenient solid-phase synthesis of tyr(3)-octreotide. Appl Radiat Isot 49(12):1581–1586. doi:10.1016/s0969-8043(98)00003-7

Lewis JS, Lewis MR, Srinivasan A, Schmidt MA, Wang J, Anderson CJ (1999) Comparison of four Cu-64-labeled somatostatin analogues in vitro and in a tumor-bearing rat model: evaluation of new derivatives for positron emission tomography imaging and targeted radiotherapy. J Med Chem 42(8):1341–1347. doi:10.1021/jm980602h

Liu S, Edwards DS (1999) Tc-99m-labeled small peptides as diagnostic radiopharmaceuticals. Chem Rev 99(9):2235–2268. doi:10.1021/cr980436l

Liu S, Edwards DS, Barrett JA (1997) Tc-99m labeling of highly potent small peptides. Bioconjug Chem 8(5):621–636. doi:10.1021/bc970058b

Maina T, Nock B, Nikolopoulou A, Sotiriou P, Loudos G, Maintas D, Cordopatis P, Chiotellis E (2002) Tc-99m demotate, a new Tc-99m-based Tyr(3) octreotate analogue for the detection of somatostatin receptor-positive tumours: synthesis and preclinical results. Eur J Nucl Med Mol Imaging 29(6):742–753. doi:10.1007/s00259-002-0782-9

Maina T, Nock BA, Cordopatis P, Bernard BF, Breeman WAP, van Gameren A, van den Berg R, Reubi JC, Krenning EP, de Jong M (2006) Tc-99m Demotate 2 in the detection of sst(2)-positive tumours: a preclinical comparison with In-111 DOTA-tate. Eur J Nucl Med Mol Imaging 33(7):831–840. doi:10.1007/s00259-006-0068-8

Melacini G, Zhu Q, Goodman M (1997) Multiconformational NMR analysis of sandostatin (octreotide): equilibrium between beta-sheet and partially helical structures. Biochemistry 36(6):1233–1241. doi:10.1021/bi962497o

Mitra S, Banerjee TS, Hota SK, Bhattacharya D, Das S, Chattopadhyay P (2011) Synthesis and biological evaluation of dibenz [b,f]

[1,5] oxazocine derivatives for agonist activity at kappa-opioid receptor. Eur J Med Chem 46(5):1713–1720. doi:10.1016/j.ejmech.2011.02.024

Nikolopoulou A, Nock BA, Maina T (2006) Tc-99m targeting of Sst(2)-expressing tumors by tetraamine-octreotide: first results in CA20948 cells and rat models. Anticancer Res 26(1A):363–366

Reubi JC, Waser B, Schaer JC, Laissue JA (2001) Somatostatin receptor sst1-sst5 expression in normal and neoplastic human tissues using receptor autoradiography with subtype-selective ligands. Eur J Nucl Med 28(7):836–846. doi:10.1007/s002590100541

Rodziewicz-Motowidio S, Brzozowski K, Legowska A, Liwo A, Silbering J, Smoluch M, Rolka K (2002) Conformational solution studies of neuropeptide gamma using CD and NMR spectroscopy. J Pept Sci 8(5):211–226. doi:10.1002/psc.384

Storch D, Behe M, Walter MA, Chen JH, Powell P, Mikolajczak R, Macke HR (2005) Evaluation of Tc-99m/EDDA/HYNIC0 octreotide derivatives compared with In-111-DOTA(0), Tyr(3), Thr(8) octreotide and In-111-DTPA(0) octreotide: does tumor or pancreas uptake correlate with the rate of internalization? J Nucl Med 46(9):1561–1569

Thakur ML, Kolan H, Li J, Wiaderkiewicz R, Pallela VR, Duggaraju R, Schally AV (1997) Radiolabeled somatostatin analogs in prostate cancer. Nucl Med Biol 24(1):105–113. doi:10.1016/s0969-8051(96)00180-1

Vaidyanathan G, Friedman HS, Affleck DJ, Schottelius M, Wester HJ, Zalutsky MR (2003) Specific and high-level targeting of radiolabeled octreotide analogues to human medulloblastoma xenografts. Clin Cancer Res 9(5):1868–1876

von Guggenberg E, Penz B, Kemmler G, Virgolini I, Decristoforo C (2006) Comparison of different methods for radiochemical purity testing of [Te-99m-EDDA-HYNIC-D-Phe(1), Tyr(3)]-octreotide. Appl Radiat Isot 64(2):194–200. doi:10.1016/j.apradiso.2005.07.019

Weiner RE, Thakur ML (2002) Radiolabeled peptides in the diagnosis and therapy of oncological diseases. Appl Radiat Isot 57(5):749–763. doi:10.1016/s0969-8043(02)00192-6

Wild D, Schmitt JS, Ginj M, Macke HR, Bernard BF, Krenning E, de Jong M, Wenger S, Reubi JC (2003) DOTA-NOC, a high-affinity ligand of somatostatin receptor subtypes 2, 3 and 5 for labelling with various radiometals. Eur J Nucl Med Mol Imaging 30(10):1338–1347. doi:10.1007/s00259-003-1255-5